The Copper Binding Domain of SPARC Mediates Cell Survival *in Vitro* via Interaction with Integrin β1 and Activation of Integrin-linked Kinase*

Matt S. Weaver[‡]**, Gail Workman**[‡]**, and E. Helene Sage**[‡§1]

From the ‡*Hope Heart Program, Benaroya Research Institute at Virginia Mason, Seattle, Washington 98101-2795 and*
§*Department of Biological Structure, University of Washington, Seattle, Washington 98195*

Secreted protein acidic and rich in cysteine (SPARC) is important for the normal growth and maintenance of the murine lens. SPARC-null animals develop cataracts associated with a derangement of the lens capsule basement membrane and alterations in lens fiber morphology. Cellular stress and disregulation of apoptotic pathways within lens epithelial cells (LEC) are linked to cataract formation. To identify molecular targets of SPARC that are linked to this disorder, we stressed wild-type (WT) and SPARC-null LEC by serum deprivation or exposure to tunicamycin. SPARC enhanced signaling by integrin-linked kinase (ILK), a serine/threonine kinase known to enhance cell survival *in vitro*. In response to stress, an ILK-dependent decrease in apoptosis was observed in WT relative to SPARC-null LEC. Co-immunoprecipitation and cross-linking of cell lysates revealed enhanced levels of a SPARC-integrin β1 complex during stress. Competition with monoclonal antibodies and peptides indicated that the copper binding domain of SPARC is required for SPARC-mediated response to stress. Inhibiting the binding and/or activity of ILK, integrin β1, or SPARC resulted in increased apoptosis of stressed LEC. We conclude that SPARC protects cells from stress-induced apoptosis *in vitro* via an interaction with integrin β1 heterodimers that enhances ILK activation and pro-survival activity.

SPARC (secreted protein acidic and rich in cysteine),[2] a member of the matricellular family of proteins, is important for the development of the murine lens and the maintenance of its transparency. SPARC-null mice develop early onset cataracts due in part to aberrant assembly of the lens capsule and disruption of fiber cells (1–5). SPARC-null mice also show accelerated wound closure (6–8), enhanced tumor growth (9–11), increased adipogenesis (12, 13), and altered extracellular matrix (ECM) deposition in a variety of tissues. A secreted glycoprotein, SPARC binds to several integral components of the ECM and exhibits an anti-adhesive function that includes abrogation of focal adhesions and disruption of cell spreading and motility (14, 15).

SPARC has traditionally been described as a stress-response protein secreted at high levels by cultured cells (16–18). However, little is known about the role secreted SPARC plays during cellular stress. SPARC has been shown to act as a survival factor in stressed glioma cells (19, 20) and to potentiate the invasiveness of certain cancers. Recent work has shown that SPARC regulates cellular assembly of fibronectin by its stimulation of the activity of integrin-linked kinase (ILK) (20, 21). Whereas ILK, by virtue of its interaction with integrin cytoplasmic domains, has been located predominantly on the cytoplasmic side of the plasma membrane, secreted SPARC acts extracellularly at points of integrin-ECM interaction. The juxtaposition of ILK and SPARC across the cell membrane necessitates the involvement of transmembrane proteins for SPARC-mediated alteration of ILK activity. The integrin receptors are logical candidates, as they have been shown previously to interact with ILK and are major mediators of signal transduction between cells and the ECM.

ILK interacts with the cytoplasmic tails of the integrin β1/β3 subunits, which play a significant role in cell adhesion, motility, differentiation, and survival (for review, see Ref. 22) and with the intracellular complex associated with focal adhesions. ILK functions downstream and independently of phosphatidylinositol 3-kinase (PI3K) to phosphorylate several effector proteins including Akt, glycogen synthase kinase 3β, the forkhead transcription factor, and integrins β1/β3. Interaction between integrins and certain ECM ligands activates ILK via the integrin cytoplasmic tail. However, little is known about the role matricellular proteins play in the initiation or modulation of ILK signaling by virtue of their alteration of integrin-ECM interaction.

Although SPARC has been shown to interact with ECM proteins and to be taken up by cells in culture, a high affinity cell surface receptor for SPARC has not been found. Stabilin-1, a scavenger receptor on alternately activated macrophages, binds SPARC specifically (23, 24) and has been proposed to facilitate macrophage-mediated clearance of SPARC from damaged tissues (23). However, with its lineage-limited expression, stabi-

[1] To whom correspondence should be addressed: 1201 Ninth Ave., Seattle,
  WA 98101-2795; Fax: 206-341-1375; E-mail: hsage@benaroyaresearch.org.

[2] The abbreviations used are: SPARC, secreted protein acidic and rich in cysteine; hSPARC, human SPARC; PI3K, phosphatidylinositol 3-kinase; rb, rabbit; ms, mouse; Ab, antibody; gt, goat; ECM, extracellular matrix; ILK, integrin-linked kinase; LEC, lens epithelial cells; MBP, myelin basic protein; ROS, reactive oxygen species; UPR, unfolded protein response; WT, wild type; mAb, monoclonal antibody; FBS, fetal bovine serum; GAPDH, glyceraldehyde-3-phosphate dehydrogenase; HRP, horseradish peroxidase; BiP, rb anti-heavy chain-binding protein; PBS, phosphate-buffered saline; dk, donkey.

lin-1 seems unlikely to mediate signaling initiated by SPARC in epithelial, endothelial, and fibroblastic cells.

We hypothesized that, during the induction of stress in cultured cells, SPARC acts as a pro-survival factor at least in part by its augmentation of ILK activity through an interaction with specific integrins. By comparing lens epithelial cells (LECs) derived from WT and SPARC-null mice, we now show that SPARC decreases apoptosis in cultured cells subjected to different types of stress and that this activity resides in the Cu^{2+} binding domain of SPARC. A SPARC-dependent increase in ILK activity was required for the enhanced survival of WT LEC, whereas inhibition of ILK resulted in increased cellular apoptosis. SPARC showed a significantly increased interaction with integrin β1 in cells subjected to stress, and this interaction was decreased after the addition of blocking antibodies against either integrin β1 or to SPARC, concomitant with decreases in ILK activity and subsequent cell death.

EXPERIMENTAL PROCEDURES

Antibodies—For immunoblotting, immunoprecipitation, and immunostaining procedures, the following antibodies were used: hamster anti-integrin β1 (Santa Cruz Biotechnology, Santa Cruz, CA), rabbit (rb) anti-integrin β1 (Upstate Cell Signaling, Lake Placid, NY), hamster integrin β1-blocking antibody (BD Biosciences), mouse (ms) monoclonal (mAb) anti-integrin α6β1/4 (Chemicon, Temecula, CA), goat (gt) anti-mouse SPARC (R&D Systems, Minneapolis, MN), ms mAb and rb polyclonal anti-ILK (Upstate), rb anti-ILK IgG (25), rb anti-caspase-3 (Cell Signaling Technology, Beverly, MA), rb anti-phospho-glycogen synthase kinase 3β (Cell Signaling Technology), ms mAb anti-glyceraldehyde-3-phosphate dehydrogenase (GAPDH) (Ambion Inc., Austin, TX), ms mAb anti-phospho-myelin basic protein (MBP) (horseradish peroxidase (HRP)-conjugate) (Upstate), and rb anti-heavy chain-binding protein (BiP) (Cell Signaling Technology). For immunoprecipitation of ILK, SPARC-blocking assays, and epitope determination, our mAbs 236, 255, 293, and 303 against human (h) SPARC, rb serum against SPARC peptide 2.1, rb serum against SPARC peptide 3.2, and guinea pig serum against SPARC peptide 2.3 were used as previously described (25–28). Rabbit polyclonal antibodies from our laboratory against ILK and SPARC were affinity-purified against their respective immunogens (25–27).

Cell Culture—C57Bl6/J × 129SVJ murine LEC were generated from lens epithelial explants as described previously (29). WT and SPARC-null mouse LEC were cultured in growth medium consisting of Dulbecco's modified Eagle's medium and 10% fetal bovine serum (FBS), 10 units/ml penicillin G, 10 μg/ml streptomycin sulfate, and 0.25 μg/ml Fungizone® (Invitrogen). Cells were released with trypsin, seeded at 1.8×10^4 cells/cm^2 on tissue culture plastic, and incubated at 37 °C with 5% CO_2 for 24 h before stress induction. Tunicamycin-treated cells were incubated for 24 or 48 h in growth medium containing 5 μg/ml tunicamycin (Calbiochem). Serum-deprived cells were incubated for 48 h in growth medium lacking FBS but containing 0.1% BSA. Control cells were incubated in growth medium only and received fresh medium at the same time as their experimental counterparts.

Immunoblotting—Control, serum-deprived, and tunicamycin-treated cells were washed with PBS, lysed with ILK lysis buffer (1% Nonidet P-40, 50 mM HEPES, 150 mM NaCl, 5 mM Na_3VO_4, 5 mM NaF, 400 μg/ml DNase, and Halt protease inhibitor mixture (Pierce)), and resolved by SDS-PAGE on 12% acrylamide gels. Proteins were transferred to polyvinylidene difluoride membranes (Millipore Corp., Billerica, MA). Nonspecific binding was blocked by incubation for 18–20 h at 4 °C in AquaBlock (East Coast Biologics, North Berwick, ME) diluted 1:1 with PBS containing 0.4% Tween 20. Membranes were incubated for 20 h at 4 °C in rb anti-BiP IgG (1:1000), gt anti-mouse SPARC IgG (1 μg/ml), ms anti-ILK IgG$_{2b}$ (1 μg/ml), rb anti-phospho-glycogen synthase kinase 3β IgG (1:1000), rb anti-caspase-3 IgG (1:1000), or ms anti-GAPDH IgG$_1$ (1 μg/ml). Blots were washed 3×5 min in PBS containing 0.4% Tween 20 and incubated for 1 h in HRP-conjugated secondary antibody (donkey (dk) anti-rabbit IgG (Jackson Immuno-Research, West Grove, PA), dk anti-goat IgG (Jackson ImmunoResearch), or gt anti-mouse IgG (Pierce). Immobilon Western HRP substrate (Millipore) was used for detection of antibody-antigen complexes. Some blots were subsequently regenerated in Restore Western blot Stripping Buffer (Pierce) according to the manufacturer's instructions and were blocked and re-probed as described above.

Measurement of Reactive Oxygen Species—Levels of cytosolic reactive oxygen species (ROS) in tunicamycin-treated WT and SPARC-null LEC were assessed as previously described (30) with slight modification. After a 24- or 48-h incubation with 5 μg/ml tunicamycin, 1 μg/ml 2′,7′-dichlorodihydrofluorescein diacetate (H_2-DCFH-DA) (Invitrogen) was incubated with the cells for 20–30 min followed by counting of fluorescent cells by flow cytometry (FACSCalibur, BD Biosciences).

Quantification of Cell Death—For analysis with acridine orange/ethidium bromide, procedures were followed as described previously (31) with some modification. Briefly, WT and SPARC-null LEC, grown for 24 h on glass coverslips in Dulbecco's modified Eagle's medium containing 10% FBS, were either deprived of serum (3 or 6 days) or exposed to tunicamycin (5 μg/ml for 24 or 48 h). Cells were incubated for 30 min at 37 °C in Dulbecco's modified Eagle's medium, FBS containing 100 μg/ml acridine orange and 100 μg/ml ethidium bromide. Cells were photographed with a fluorescence microscope (Leica Microsystems AG, Wetzlar, Germany) and were scored as follows: full green nuclei, viable cells; condensed green nuclei, early mid apoptotic cells; condensed red nuclei, mid-late apoptotic cells; full red nuclei, necrotic cells. Routinely 3–4 panels containing 250–300 cells each were counted per condition. Additionally, the viability of trypsinized cells was determined by trypan blue exclusion.

Immunoprecipitation—Control, serum-deprived, and tunicamycin-treated cells were washed with PBS and were lysed with ILK lysis buffer as described above. As controls for immunoprecipitation in each trial, experimentally treated lysates were precipitated with beads only and a nonspecific antibody. Resulting immunoblots from these samples was negative unless otherwise indicated in each figure. For blocking experiments, 10 μg/ml nonspecific ms IgG, ms integrin β1-blocking antibody, or ms anti-SPARC mAb (236, 255, 293, or 303) was added

to the media during induction of stress. Lysates were collected, and protein concentration was determined by BCA assay (21). Two μg of hamster anti-integrin $\beta1$ IgG, ms anti-integrin $\alpha6\beta1/4$ IgG, or rb polyclonal antibody anti-ILK (25) was added to 150–200 μg of total cell lysates, and incubation occurred with gentle agitation for 20 h at 4 °C. Twenty μl of protein A/G$^+$-agarose (Santa Cruz Biotechnology) was added to each sample, and incubation was continued for 1 h at 4 °C with agitation. Samples were purified by 2 sequential washes with ILK lysis buffer (modified to contain 750 mM NaCl) and boiled for 10 min in SDS-PAGE buffer (21) containing 1 mM dithiothreitol. Samples were centrifuged at 10,000 rpm for 5 min at room temperature before resolution by SDS-PAGE. Immunoblots were incubated for 20 h at 4 °C in gt anti-mouse SPARC IgG (1 μg/ml), and protein detection was performed as described above.

ILK Activity Assay—Immunoprecipitation of ILK from serum-deprived or tunicamycin-treated LEC was carried out as detailed above. For blocking experiments, 10 μg/ml integrin $\beta1$-blocking antibody (BD Biosciences), ILK inhibitor KP-392 (a gift from Dr. Shoukat Dedhar), or the PI3K-inhibitor LY294002 (Cell Signaling Technology, final concentration 10 μM) was added to cells during stress induction. Normal rb IgG (Jackson ImmunoResearch) was used to control for nonspecific antibody interactions. Immune complexes were isolated by a 1-h incubation with protein A/G$^+$-agarose at 4 °C followed by 2 washes with ILK wash buffer and two washes with ILK kinase buffer (50 mM HEPES, 5 mM Na$_3$VO$_4$, 5 mM NaF, 10 mM MgCl$_2$, 2 mM MnCl$_2$). For kinase reactions, samples were incubated at 30 °C for 25 min in ILK kinase buffer containing 200 mM ATP and 5 μg/ml MBP. Samples were boiled in SDS-PAGE buffer with 1 mM dithiothreitol for 10 min, centrifuged at room temperature for 5 min at 10,000 rpm, and resolved by SDS-PAGE. Proteins were transferred as above, and phosphorylated MBP was detected with HRP-conjugated ms anti-phospho-MBP (21).

Altered Media Renewal—WT LEC were incubated for 24 h with 5 μg/ml tunicamycin. LEC were incubated normally for the initial 12 h. For the subsequent 12 h, every 2–3 h, all of the conditioned media was removed, the cells were washed with PBS, and either the conditioned media (SPARC-null or WT) or fresh media were added back to the cells. Cells were lysed and immunoprecipitated as described above. WT LEC not receiving media renewal were used as a positive control.

Protein Cross-linking—During a 24-h incubation, control and tunicamycin-treated cells were labeled with UV-sensitive amino acid derivatives L-photo-Leucine and L-photo-methionine according to the manufacturer's instructions (Pierce). Cells were washed with PBS and UV-cross-linked for 10 min in a UV Stratalinker 1800 (Stratagene, La Jolla, CA) at 365 nm. Cells were subsequently lysed in ILK lysis buffer as described above. SDS-PAGE was performed as described above, with the following modifications; samples were reduced and run on a 3–8% Tris acetate NuPage™ Novex™ minigel (Invitrogen).

Epitope Determination—mAbs raised against recombinant human SPARC were selected for their reactivity with both hSPARC and msSPARC. Epitopes of the four chosen

mAbs were mapped by enzyme-linked immunosorbent assay against a library of SPARC peptides consisting of overlapping 10-mers homologous to hSPARC, with an overlap of 3 residues. The 91 overlapping SPARC peptides plus 5 non-SPARC 10-mers were synthesized and covalently bound to "pins" by Mimotopes International (Clayton, Victoria, Australia) according to their Multipin™ synthesis platform. The rack of 96 pins, arranged in an 8 × 12 array, allowed immersion of the peptide-bearing pins into the wells of enzyme-linked immunosorbent assay plates containing antibody or substrate solutions.

Enzyme-linked immunosorbent assays were performed according to the manufacturer's instructions. Briefly, the rack of pins (the peptide array) was blocked for 1 h in PBS containing 2% casein acid hydrolysate (Sigma-Aldrich) and 0.1% Tween 20, washed 3 × 10 min in PBS, incubated for 1 h in anti-SPARC mAb at 0.5 μg/ml in antibody diluent (PBS containing 0.1% BSA or casein acid hydrolysate, 0.1% Tween 20), washed 3 × 10 min in wash buffer (PBS, 0.1% Tween 20), incubated in peroxidase-labeled gt anti-ms IgG (secondary) (KPL, Gaithersburg, MD) at 0.2 μg/ml in antibody diluent, washed 3 × 10 min in wash buffer, and immersed in TMB substrate (OptEIA™, BD Biosciences). Assays testing the binding of the secondary alone were used to control for background reactivity. Color development was stopped at 1.5 min (mAb 255), 3 min (mAb 293), or 10 min (mAb 236, mAb 303, and secondary antibody alone); absorbance was recorded at 450 nm. The peptide array was regenerated by ultrasonication in 10× PBS containing 1% SDS and 0.1% β-mercaptoethanol.

Each antibody was assayed three times. The 96 absorbance readings from each assay were scaled from 0 to 1 for analysis. The average of the control assays (the secondary alone) was calculated and subtracted from each mAb anti-SPARC data point.

Dot Blot Analysis—Two μl of a 4 mM stock solution of SPARC peptides (2.1, 2.3, 3.2, and Z-2) (26, 27, 32) in PBS was spotted on a pre-wetted polyvinylidene difluoride membrane and allowed to dry. The membrane was subsequently blocked and probed as described above with 1 μg/ml nonspecific ms IgG or anti-SPARC mAb (236, 255, 293, or 303). To validate the reactivity of spotted peptides, we independently probed the membrane with a 1:1000 dilution of anti-peptide 2.1 (rb), anti-peptide 2.3 (guinea pig), or anti-peptide 3.2 (rb) (26, 27).

SPARC Peptide Competition—Control (48 h), serum-deprived (48 h), and tunicamycin-treated (24 h) cells were incubated with varying concentrations of SPARC peptides 2.3 or 1.1 (9, 27, 32). After the incubation, cells were washed with PBS and lysed with ILK lysis buffer, and lysates were immunoprecipitated as described above.

Exogenous Murine SPARC Addition—Medium conditioned by WT LEC was determined to contain ~13.5 nM SPARC by comparative immunoblot analysis (data not shown). SPARC-null LEC were incubated with and without stress conditions in WT-conditioned media, serially diluted with SPARC-null-conditioned media to contain 0–13.5 nM murine SPARC. After incubation, cells were washed with PBS and lysed with ILK lysis
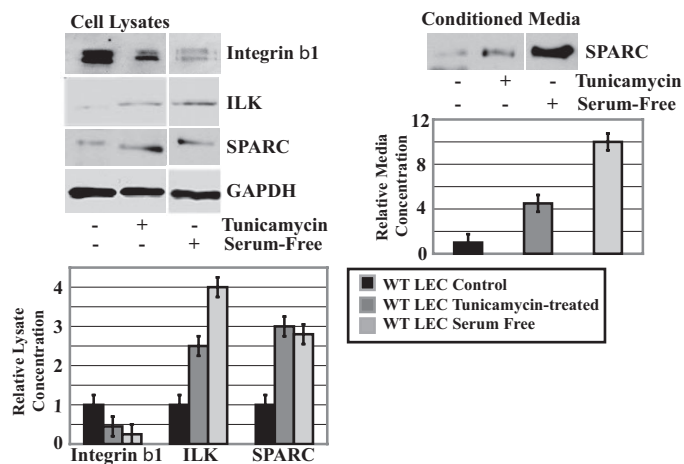
FIGURE 1. **SPARC is increased in WT LEC during cellular stress.** WT LEC were either serum-deprived (48 h) or exposed to 5 μg/ml tunicamycin (24 h). Protein from total cell lysates (20 μg/lane) and conditioned media (volume determined by relative protein concentration from lysates) were immunoblotted for SPARC, ILK, and integrin β1. Composite blots are from single membranes and are representative of three independent experiments. GAPDH was probed as a loading control.

buffer, and lysates were immunoprecipitated as described above.

RESULTS

SPARC Is Increased during Stress—The expression of SPARC increases as cells adapt to culture or are subjected to different forms of stress (16). To determine the role of SPARC in cell survival, we stressed LEC isolated from WT and SPARC-null mice by serum deprivation. In parallel, the inhibitor of dolichol-phosphate-mediated *N*-glycosylation, tunicamycin, was used to initiate an intracellular stress response, as previous work has shown that the administration of tunicamycin to LEC results in an endoplasmic reticulum-associated unfolded protein response (UPR) (30).

In culture, LEC produce and secrete SPARC into their media. When placed under stress conditions, cell-associated and secreted SPARC protein levels were increased relative to unstressed control cells (Fig. 1). ILK levels also were increased in response to stress, whereas integrin β1 appeared to decrease. Conditioned media were probed additionally for ILK, integrin β1, and GAPDH, with no reactivity (data not shown).

WT and SPARC-null LEC Undergo UPR—UPR is characterized by increased levels of ROS, the endoplasmic reticulum chaperone BiP, and caspase 3 and 12 activation as well as induction of apoptosis (for review, see Ref. 33). To characterize the UPR in the presence or absence of SPARC, we treated LEC with tunicamycin and assayed for levels of ROS or BiP. After the addition of redox-reactive dye, LEC were analyzed by flow cytometry. ROS levels in LEC increased over time after exposure to tunicamycin (Fig. 2, *panels A and B*). SPARC-null LEC consistently showed ROS levels higher than those of WT LEC before and during the addition of tunicamycin ($p < 0.05$). As an additional indicator of UPR induction, levels of BiP were determined by immunoblotting (Fig. 2C). Both SPARC-null and WT LEC displayed an ~4-fold induction of BiP after exposure to tunicamycin. Neither intracellular ROS nor BiP induction was observed as a
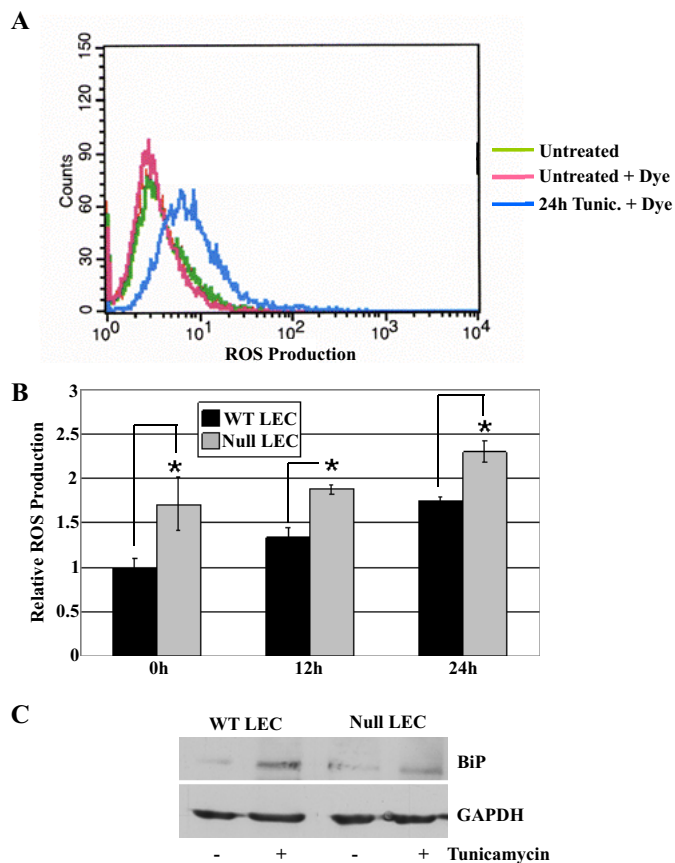

FIGURE 2. **The UPR response in WT and SPARC-null LEC.** WT and SPARC-null LEC were exposed to tunicamycin (5 μg/ml) for 0, 12, or 24 h. *A*, representative flow cytometry of untreated cells or cells treated 24 h with tunicamycin (*Tunic.*) and subsequently incubated with 2′,7′-dichlorodihydrofluorescein diacetate dye to show ROS production. *B*, quantified ROS production from flow cytometry after exposure of LEC to tunicamycin (*, $p < 0.05$). *Bars* represent the mean of three independent experiments $\pm$ S.D. *C*, immunoblot of UPR-induced protein BiP in resting and tunicamycin-treated LEC. Blots were subsequently probed with GAPDH to evaluate protein loading. The blot shown is representative of three independent experiments.

consequence of serum deprivation (data not shown). Based on elevated ROS and BiP levels, both SPARC-null and WT LEC were shown to generate a UPR after exposure to tunicamycin.

SPARC Protects LEC against Apoptosis in Vitro—Fig. 3 shows the levels of SPARC in response to the two different types of stress. As expected, SPARC-null LEC exhibited no SPARC, whereas SPARC protein in WT LEC was increased after serum deprivation or exposure to tunicamycin (5- and 4-fold, respectively) (Fig. 3, *panels A and D*). LEC were also stained with trypan blue or a combination of ethidium bromide/acridine orange, the former to determine total cell death after the induction of stress (Fig. 3, *panels B and E*), whereas the latter was diagnostic for apoptosis by nuclear condensation and permeability (31, 34) (Fig. 3, *panels C and F*). Comparable staining with trypan blue and ethidium bromide/acridine orange indicated that stress-induced cell death in the two LEC populations occurs primarily through apoptotic pathways. In both serum-free and tunicamycin-supplemented culture media, SPARC-null LEC showed significantly increased rates of apoptosis in comparison with WT LEC.
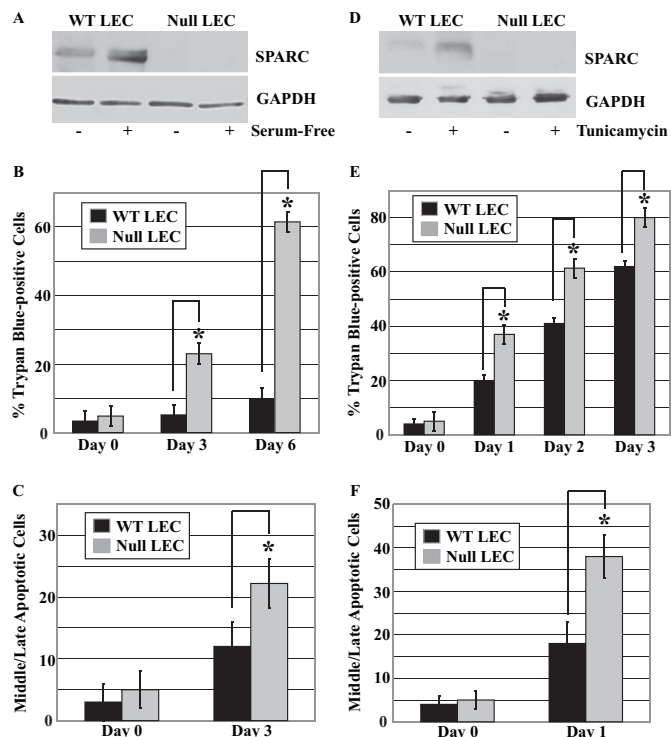
FIGURE 3. **Anti-apoptotic activity of SPARC during stress *in vitro*.** WT and SPARC-null LEC were either serum-deprived or exposed to tunicamycin (5 μg/ml) for the times indicated. *A*, immunoblot of SPARC in total cell lysates after 48h of serum deprivation. *B*, quantification of total cell death in serum-deprived LEC by trypan blue inclusion (*, $p < 0.02$). *C*, quantification of apoptosis induced by serum deprivation by examination of nuclei stained with ethidium bromide/acridine orange (*, $p < 0.02$). *D*, immunoblot of SPARC in total cell lysates after 24h of exposure to tunicamycin. *E*, quantification of total cell death in tunicamycin-treated LEC by trypan blue inclusion (*, $p < 0.05$). *F*, quantification of apoptosis induced by tunicamycin by examination of nuclei stained with ethidium bromide/acridine orange (*, $p < 0.05$). GAPDH was used as a protein loading control for immunoblots. *A* and *D* are representative of three independent experiments. *Columns* in *B*, *C*, *E*, and *F* represent the mean of three independent experiments ±S.D.

PI3K-dependent ILK Activity Is Affected by SPARC—As a survival factor, ILK has been shown to phosphorylate directly several downstream activator molecules and, indirectly, to affect the activity of several pro-/anti-apoptotic proteins. ILK interacts directly with Akt, glycogen synthase kinase 3β, and the forkhead transcription factor (22). Additional apoptosis-associated proteins affected by ILK include caspase-3, caspase-9, and Bcl-2 family members. As shown in Fig. 4, immunoblotting and *in vitro* kinase assays were performed to determine the relative level and activity of ILK and its PI3K dependence in WT and SPARC-null LEC. To determine ILK response during stress, we performed immunoblots with lysates from resting and stressed LEC (Fig. 4*A*). Both WT and SPARC-null LEC demonstrated increased ILK production during stress. For ILK activity in resting and stressed LEC, with and without exposure to the PI3K inhibitor LY294002, lysates were immunoprecipitated with anti-ILK antibodies and subjected to assays utilizing MBP as an ILK substrate. WT LEC showed increased, PI3K-dependent ILK activity when subjected to serum deprivation or tunicamycin (Fig. 4*B*). All results were normalized to the amount of ILK protein immunoprecipitated from each assay.

ILK Activity Is Required for SPARC-mediated Survival—Previous studies indicated that SPARC has an anti-apoptotic func-
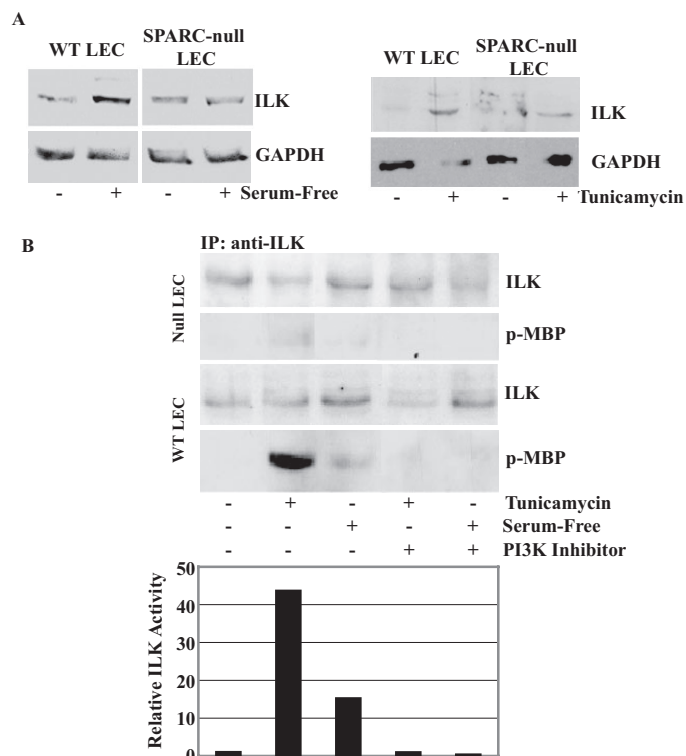

FIGURE 4. **Stress-induced ILK activity in WT LEC is PI3K-dependent.** Lysates of serum-deprived or tunicamycin-treated WT and SPARC-null LEC with and without the PI3K inhibitor LY294002 were immunoblotted or co-immunoprecipitated (*IP*) with rabbit anti-ILK antibodies and assayed for ILK activity. *A*, immunoblot analysis of LEC lysates. GAPDH was used as a protein loading control. *B*, ILK activity in stressed LEC. Relative ILK expression in WT cells under each condition was normalized to the total amount of ILK protein immunoprecipitated for each reaction. Singular and composite blots are from single membranes and are representative of three independent experiments. *p-*, phospho.

tion via its stimulation of Akt and ILK activity in gliomas (19, 20). Phosphorylated Akt is a downstream effector of the PI3K and ILK signaling pathways that promote survival. We reduced ILK activity by chemical inhibition in stressed LEC to ask whether the anti-apoptotic role of SPARC during stress is dependent on an ILK-mediated pathway.

To determine whether the increased ILK activity observed in WT LEC accounted for enhanced survival, we stressed WT and SPARC-null LEC as before but with the addition of the small molecule, ILK-specific inhibitor KP-392 (35); total cell death was calculated by inclusion of trypan blue dye. The addition of the ILK inhibitor to serum-deprived (Fig. 5*A*) or tunicamycin-treated (Fig. 5*B*) LEC elevated total death in WT LEC to levels comparable in SPARC-null cells. KP-392 added to SPARC-null LEC did not increase total cell death after induction of stress (data not shown).

Extracellular SPARC-Integrin β1 Interaction Is Enhanced during Stress—Although previous work has shown that SPARC affects ILK activity (20, 21), the mechanism for an interaction between a secreted (SPARC) and intracellular (ILK) protein has not been resolved. SPARC has also been shown to diminish focal adhesion complexes *in vitro* (14). Integrins are a primary component of focal adhesions, which enable cross-talk between the ECM and intracellular signaling molecules, *e.g.* ILK. It was, therefore, of interest to
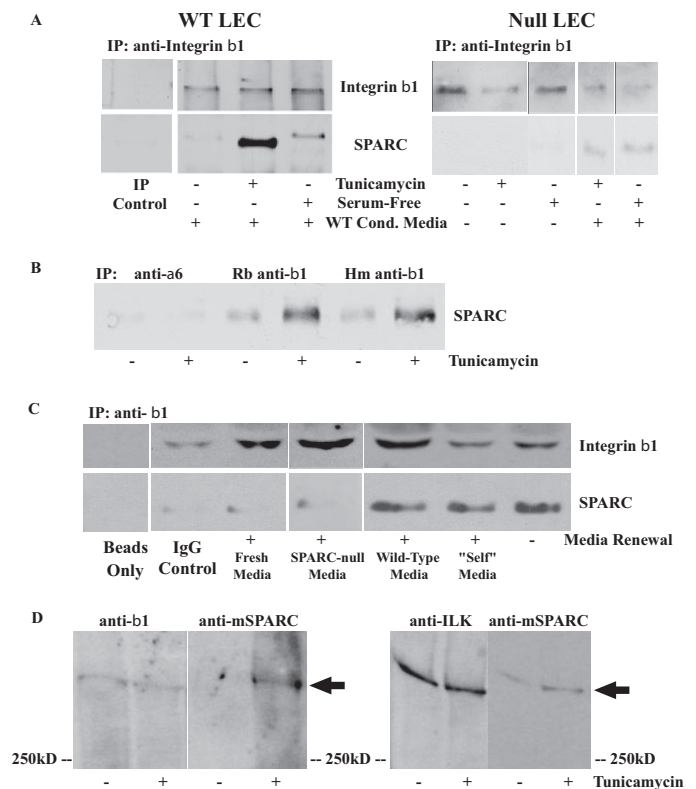
A

B
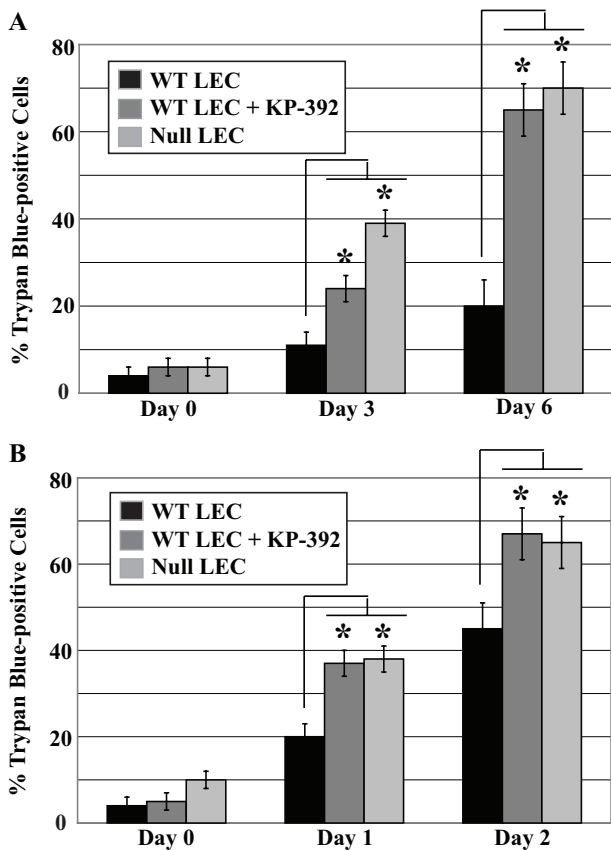
FIGURE 5. **ILK activity contributes to the survival of stressed WT LEC.** WT LEC were stressed by serum deprivation or exposure to tunicamycin (5 μg/ml) in the presence or absence of the ILK inhibitor KP-392. *A*, trypan blue inclusion in LEC after serum deprivation and addition of ILK inhibitor (*, $p < 0.02$). *B*, trypan blue inclusion in LEC after tunicamycin treatment and the addition of ILK inhibitor (*, $p < 0.05$). In *A* and *B*, each *column* represents the mean of three independent experiments ±S.D.

FIGURE 6. **Extracellular SPARC binds to β1-integrin during stress and enhances ILK activity.** Lysates of serum-deprived or tunicamycin-stressed WT and SPARC-null LEC were either used for immunoblot analysis or were immunoprecipitated (*IP*) by the following antibodies: rat or rabbit (Rb) anti-integrin β1 and rat anti-integrin $α_6β1/β_4$. Immune complexes and cross-linked proteins were probed for SPARC, ILK, and integrin β1 by immunoblot. *A*, co-immunoprecipitation of SPARC with anti-integrin β1 from LEC after serum deprivation (48 h) or tunicamycin exposure (24 h). Additionally, SPARC-null LEC were incubated with SPARC-containing media conditioned by WT LEC while serum-free or tunicamycin-exposed (*WT Cond. Medium*). *B*, co-immunoprecipitation of SPARC with various anti-integrin antibodies after tunicamycin exposure (24 h). *Hm*, hamster. *C*, co-immunoprecipitation of SPARC with anti-integrin β1 IgG from tunicamycin-exposed (24 h) LEC with and without renewal with fresh medium or SPARC-null- or WT-conditioned medium from separate cultures or WT-conditioned medium of the cells from which lysates were immunoprecipitated ("*Self*" *Medium*). *D*, immunoblot of SPARC, ILK, and integrin β1 in cross-linked protein complexes with and without tunicamycin. Singular and composite blots are from single membranes and are representative of three independent experiments.

explore the role of integrins as mediators between SPARC and ILK during stress induction in LEC.

Lysates from LEC that were serum-deprived or exposed to tunicamycin (Fig. 6*A*) were immunoprecipitated with anti-integrin β1 antibodies and were subsequently probed for SPARC. Increased levels of SPARC-integrin β1 complex were observed in WT LEC after stress induction. Additionally, a SPARC-integrin β1 complex was revealed after SPARC-null LEC were stressed in WT LEC-conditioned media containing secreted, murine SPARC (Fig. 6*A*).

To verify the apparent interaction between SPARC and integrin β1, we used several different antibodies in co-immunoprecipitation assays. Anti-$α6β1/4$ integrin antibodies did not immunoprecipitate SPARC from stressed LEC. However, multiple anti-integrin β1 antibodies, with different specificities, revealed increased SPARC-integrin β1 interaction after induction of stress (Fig. 6*B*).

Because both SPARC and integrin β1 are processed through the classical secretory pathway, interaction between the two proteins might be an intracellular process before secretion of SPARC. To address this issue, we periodically washed and subsequently incubated stressed cells with either conditioned medium or fresh medium without secreted SPARC. When cells were given SPARC-null conditioned or fresh medium, the

SPARC-integrin β1 interaction was eliminated (Fig. 6*C*) relative to the slight decrease observed in cells receiving WT-conditioned medium.

For confirmation of the formation of a complex containing SPARC, integrin β1, and ILK, cells were labeled and cross-linked with UV-sensitive amino acid derivatives. Western analysis showed the formation of a large protein complex that included ILK and integrin β1 under all conditions as well as SPARC under conditions of stress (Fig. 6*D*).

ILK-mediated Survival Is Dependent on SPARC-Integrin β1 Interaction—SPARC and integrin-blocking antibodies were added to LEC in an attempt to inhibit the interaction between SPARC and integrin β1 (Fig. 7 and Fig. 8). Nonspecific, isotype control antibodies showed no effect on SPARC-integrin β1 interaction, but the addition of integrin β1-blocking antibodies eliminated SPARC from the immunoprecipitated complexes (Fig. 7*A*). *In vitro* kinase reactions were used to determine
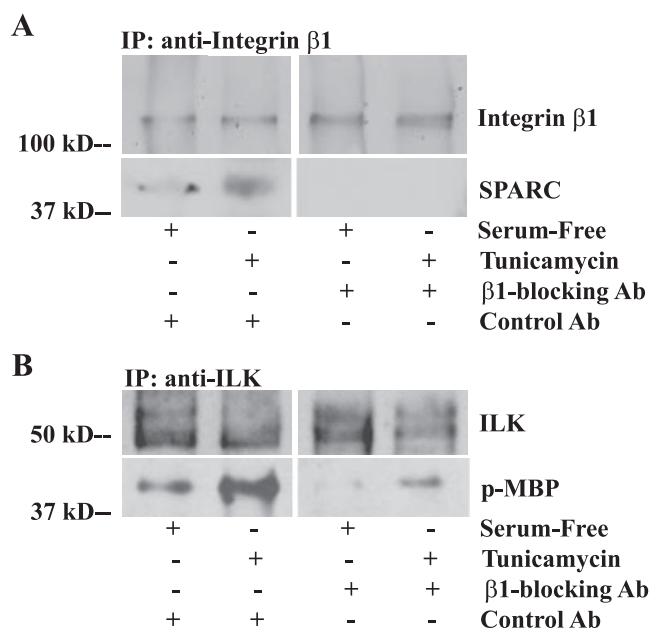
FIGURE 7. **The addition of integrin β1-blocking antibodies prevents SPARC binding and inhibits ILK signaling.** Lysates of WT LEC stressed by serum deprivation or exposure to tunicamycin in the presence of an isotype control or integrin β1-blocking antibody (10 μg/ml) were co-immunoprecipitated (*IP*) with rabbit anti-integrin β1 or rabbit anti-ILK antibody. *A*, stress-induced co-immunoprecipitation of SPARC and integrin β1 in the presence of integrin β1-blocking antibody. *B*, immunoblot of total ILK and phosphorylated (*p-*) MBP from immunoprecipitated ILK (in the presence of integrin β1-blocking antibody) from lysates of stressed WT cells. Each gel is representative of three independent experiments.

whether inhibition of the SPARC-integrin β1 interaction influenced ILK activity during stress (Fig. 7*B*). Integrin β1-blocking antibodies, also shown to block SPARC-integrin β1 complex formation, lowered ILK activity in serum-deprived or tunicamycin-treated WT LEC (Fig. 7*B*).

Anti-SPARC mAbs varied in their capacity to block the interaction of SPARC with integrin β1 (Fig. 8*A*). Total cell death, as measured by trypan blue staining, of tunicamycin-treated WT LEC was increased to levels observed in SPARC-null LEC by the addition of SPARC-blocking mAb 255 (Fig. 8*B*). In contrast, nonspecific antibodies (IgG) or a non-blocking anti-SPARC mAb (303) exhibited minimal effects on the death of WT LEC cultured in the presence of tunicamycin (Fig. 8*B*).

The Follistatin Domain of SPARC Interacts with Integrin β1—The differences between the four anti-SPARC mAbs in their capacity to block the SPARC-integrin β1 interaction prompted an investigation into the epitopes of each antibody. Potential epitopes were first identified by testing the mAbs in a series of enzyme-linked immunosorbent assays against a Multipin™ peptide array representing the full-length amino acid sequence of hSPARC. The peptide array contained 91 overlapping 10-mers homologous to hSPARC, each offset from its neighbor by 3 residues. Each mAb was assayed against the entire peptide array three separate times. Background activity of the HRP-conjugated secondary antibody alone was subtracted from each reading (Fig. 9). Potential epitopes were selected according to 1) high net reactivity with adjacent overlapping peptides, and 2) an absorbance pattern indicative of a peak (candidate peaks are circumscribed by *red boxes*, and predicted epitope sequences are shown in *red* in the *insets*, Fig. 9).
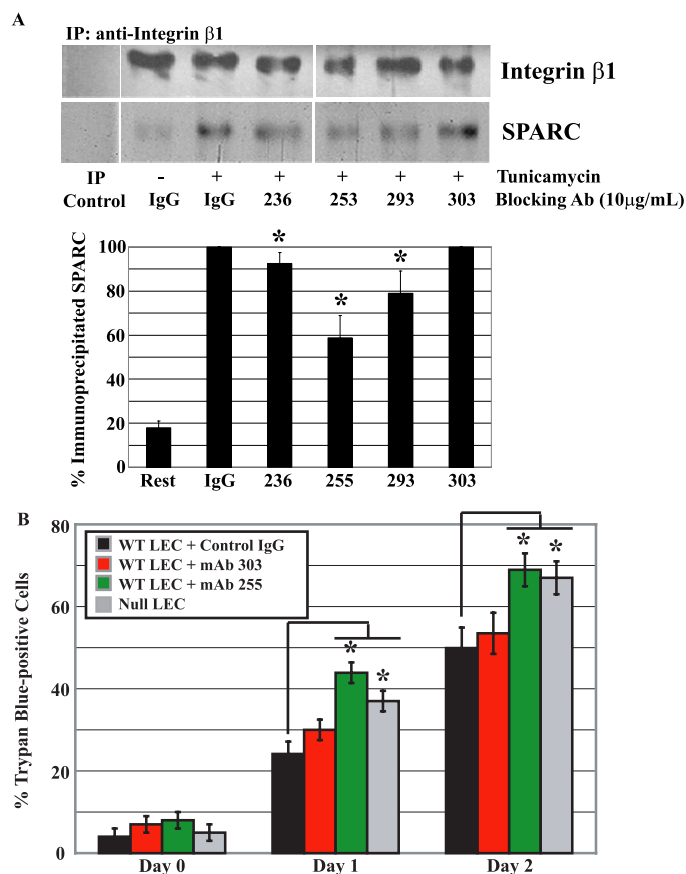
FIGURE 8. **Interaction between SPARC and integrin β1 is inhibited by several anti-SPARC mAbs.** WT LEC were exposed to tunicamycin for 24 or 48 h in the presence of 10 μg/ml nonspecific ms IgG or one of the anti-SPARC mAbs: 236, 255, 293, or 303. Relative co-immunoprecipitation (*IP*) of SPARC and integrin β1 (*A*) and total cell death (*B*) are shown. *A*, quantification of SPARC and integrin β1 co-immunoprecipitation after incubation with nonspecific IgG or anti-SPARC mAbs for 24 h. The SPARC signal (*black bars*) from the cell lysate incubated with nonspecific IgG was set at 100% (*, *p* < 0.05). *B*, trypan blue staining of tunicamycin-treated LEC (days 0, 1, and 2) incubated with IgG or anti-SPARC mAbs (*, *p* < 0.05). *A* and *B* represent the mean of three independent experiments ±S.D. The composite blot is from a single membrane and is representative of three independent experiments.

Two of the mAbs, 236 and 293, yielded multiple peaks within the N-terminal half of SPARC, indicating the possibility that the mAbs bind to peptide sequences separated by nonbinding sequences within the primary structure of SPARC but brought into spatial proximity by its tertiary structure. This supposition was borne out by reacting mAbs with soluble 20- and 50-mers approximating domains of SPARC (26, 32) (Fig. 10). Several of the peptides were dotted onto polyvinylidene difluoride membranes and probed with the four mAbs; each of these mAbs detected peptides predicted by the data from the Multipin™ assay and did not detect peptides for which there were no corresponding peaks (Figs. 9 and 10). mAbs 236 and 293 detected peptides 2.1 and 2.3 from the follistatin domain but not Z-2 from the EC domain (see Fig. 10*A* for reference). mAb 255 detected one of the 2 follistatin domain peptides (2.3), and mAb 303 detected peptide Z-2 only (Fig. 10*B*, *colored arrows* correspond to peptides shown in Fig. 10*A*).

The three mAbs with inhibitory activity toward the formation of a SPARC-integrin β1 complex all proved to have epitopes in the follistatin domain of SPARC, whereas the non-

A

mAb 236

B
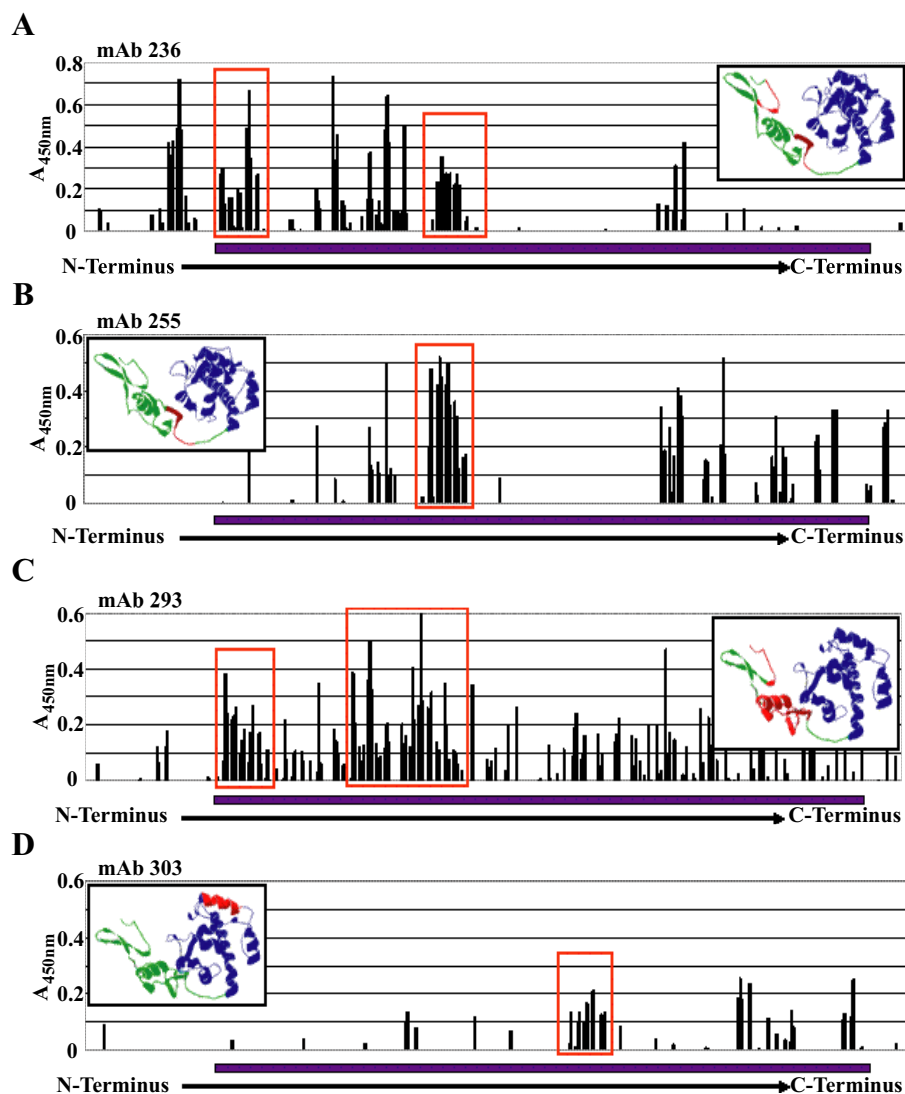

mAb 255

C

mAb 293

D

mAb 303

FIGURE 9. **Identification of epitopes recognized by anti-SPARC mAbs.** A Multipin[TM] peptide array representing the full sequence of hSPARC as contiguous and overlapping 10-mers (see "Experimental Procedures") was used to identify epitopes recognized by 4 anti-SPARC mAbs. Each graph (*A–D*) shows the reactivity of the mAb against overlapping, sequential peptides in three separate experiments. The *inset panel* displays predicted epitope position (*red*) in a molecular model of SPARC derived from A chain coordinates of Protein Bank Accession 1BMO (40). The *blue bar* along the *x* axis denotes the sequence represented in the molecular model. *A*, anti-SPARC mAb 236. *B*, anti-SPARC mAb 255. *C*, anti-SPARC mAb 293. *D*, anti-SPARC mAb 303. Potential epitopes were selected on the basis of high reactivities with contiguous peptides, and predicted epitopes are designated by *red rectangles*.

of peptide 1.1 (from domain 1 of SPARC) was predicted from the partial inhibition of SPARC anti-apoptotic activity by anti-SPARC IgG, as most antibodies against intact SPARC react strongly with domain 1.
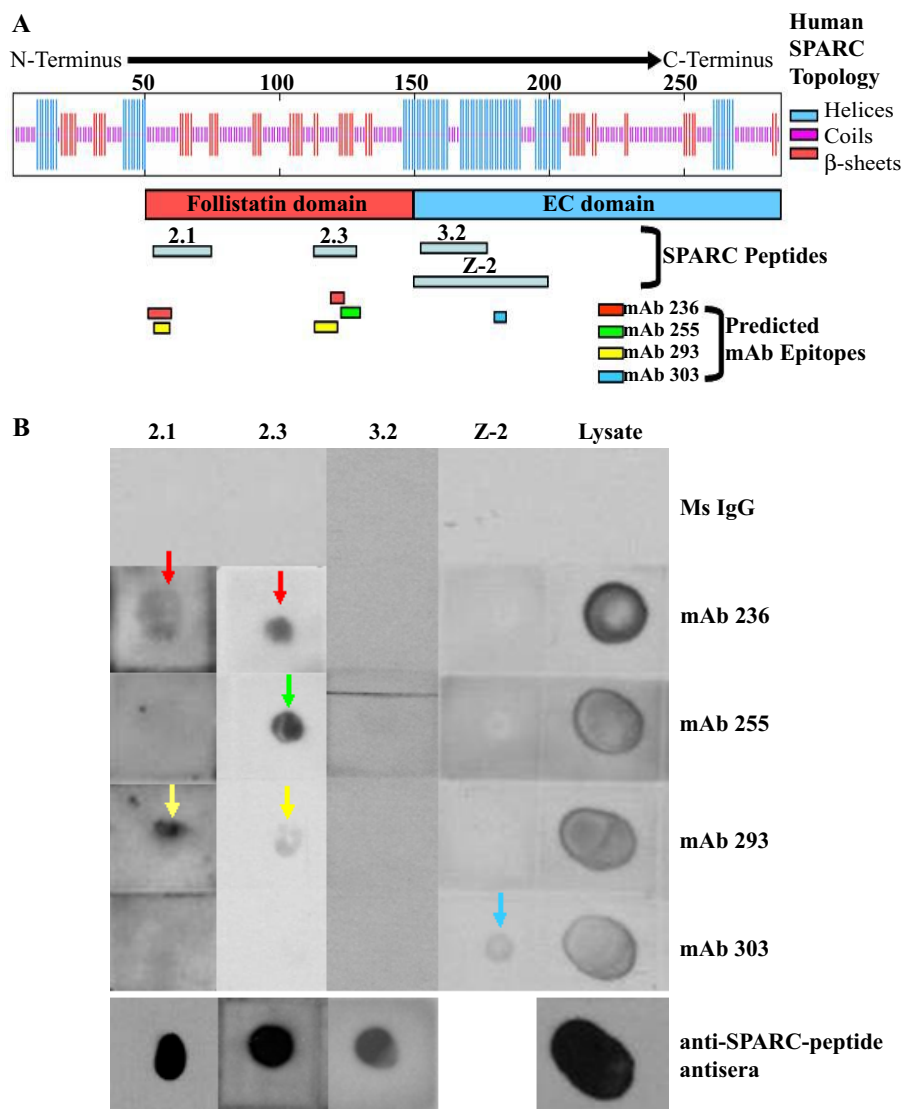
SPARC Peptide 2.3 Inhibits Extra-cellular SPARC Functions—To show the extracellular specificity of peptide competition with SPARC, we used peptide 2.3 in a series of assays with SPARC-null cells treated with exogenous SPARC from WT LEC. Co-immunoprecipitation of tunicamycin-treated SPARC-null LEC incubated with varying concentrations of murine SPARC (0–13.5 nM) revealed a concentration-dependent SPARC-integrin β1 interaction. This interaction was inhibited by the addition of peptide 2.3 to the medium (Fig. 12*A*). Peptide 2.3 also competed with SPARC on stressed WT LEC in a cross-linking experiment (Fig. 12*B*). Finally, the capacity of peptide 2.3 to inhibit a function of SPARC downstream was explored in SPARC-null LEC by an *in vitro* ILK kinase assay (Fig. 13). Whereas increasing SPARC concentrations corresponded with increased ILK activity, the addition of peptide 2.3 inhibited this function (Fig. 13).

DISCUSSION

The most striking developmental characteristic of SPARC-null mice is early onset cataractogenesis. Cataracts are generally associated with alterations in LEC behavior, lens capsule formation, deposition of

integral ECM components, and general stress responses in lens fiber cell layers (36). Several common lens pathologies result from the sensitivity of this tissue to external stressors such as hypoxia, fluctuations in ionic balance, hyperglycemia, and ultraviolet irradiation. The discovery of SPARC in our laboratory was an outcome of its production by cells *in vitro* subjected to stress, *e.g.* "culture shock" (16). Although SPARC was presented as a pro-survival factor in a recent study (20), its role in cell survival after stress induction had not been elucidated. A potential clue to a mechanism by which SPARC might regulate cell survival is its capacity to increase the activity of ILK during fibronectin assembly (21). Despite an apparent colocalization of SPARC and ILK on the surface of cells, the mechanism by which ILK activity is enhanced by SPARC is not known. We hypothesized that SPARC exhibits a pro-survival function in

inhibitory mAb 303 was found to react only with a sequence that was more C-terminal (*i.e.* in the EC domain). Furthermore, the three inhibitory mAbs (236, 255, and 293) reacted with peptides encompassing the SPARC copper binding sequence KKGHK, as shown both by the Multipin[TM] assay and by the dot blot of peptide 2.3 (Fig. 10, *panels A* and *B*, respectively).

SPARC Peptide 2.3 Inhibits SPARC-Integrin β1 Interaction—To demonstrate the specificity of the SPARC-integrin β1 interaction, we used peptide 2.3 in a series of competition assays. SPARC peptide 2.3 was shown to impair SPARC-integrin β1 interaction in a concentration-dependent manner. The capacity of peptide 2.3 to inhibit the SPARC-integrin β1 interaction was significantly greater than that seen in the presence of another SPARC peptide (1.1) of comparable size but from the N-terminal domain (Fig. 11, *panels A* and *B*). The effect

FIGURE 10. **Confirmation of epitopes predicted by Multipin™ peptide array.** SPARC peptides (20- and 30-mers) were dotted onto polyvinylidene difluoride membranes and probed with anti-SPARC mAbs 236, 255, 293, and 303. *A,* schematic diagram of SPARC showing relative positions of the portion of SPARC for which crystallographic data exist (*red bar,* follistatin domain; *blue bar,* extracellular calcium binding (*EC*) domain), SPARC peptides (*gray bars*), and mAb epitopes predicted by Multipin™ peptide array (*colored bars*). *B,* dot blot shows immunodetection by anti-SPARC mAbs of peptides containing the predicted epitopes (236, *red;* 255, *green;* 293, *yellow;* 303, *blue*). Reactivity of dotted peptides was confirmed by the use of guinea pig and rabbit antisera against the respective peptides (anti-SPARC peptide antisera). Composite blots for peptides 2.1, 2.3, 3.2, and Z-2 are from single membranes and are representative of three separate experiments.
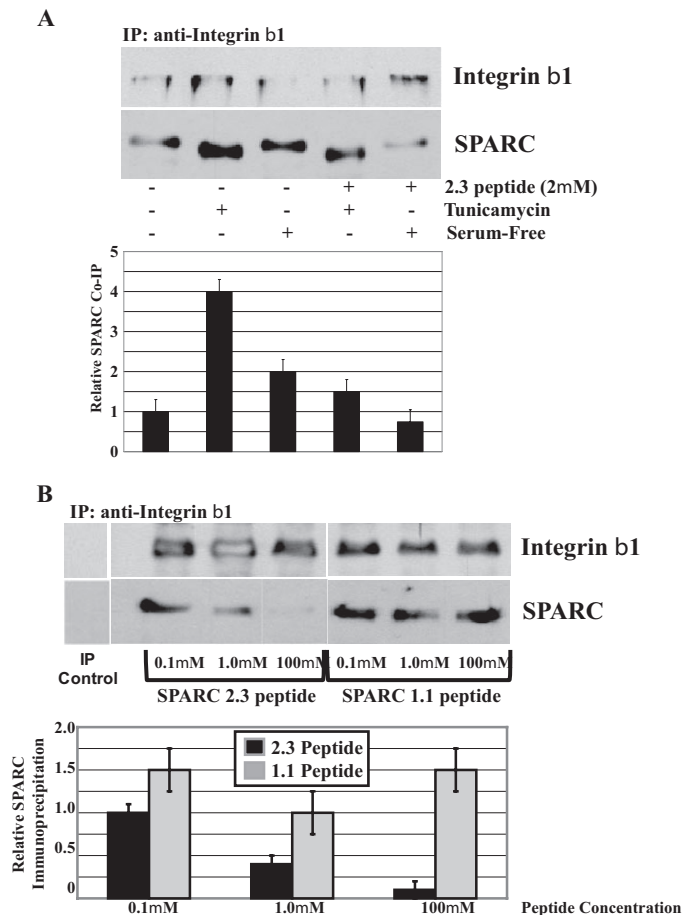
immunoprecipitations with anti-integrin antibodies showed integrin β1 protein levels equivalent to those in resting cells, results allowing reasonable estimates of SPARC interaction (Figs. 6–8).

Before secretion, SPARC is prominent in the endoplasmic reticulum and has been proposed as a molecular chaperone that guides the folding of basement membrane proteins (37). Emerson *et al.* (38) have recently demonstrated that SPARC acts as a chaperone on model protein substrates. It was, therefore, of interest to generate endoplasmic reticular stress and the subsequent UPR in WT and SPARC-null cells. Survival after the UPR is dependent on endoplasmic reticulum-specific chaperone activity and is causally related to cataract formation in the lens (30). As indicated by increased ROS and BiP production, both WT and SPARC-null LEC undergo an UPR after overnight exposure to the inhibitor of *N*-glycosylation, tunicamycin (Fig. 2). There is a slight increase in ROS production and a reduced induction of BiP in SPARC-null LEC, the data indicating a possible role for SPARC during the UPR and correlating with elevated apoptosis in SPARC-null LEC.

For comparison with the intracellular effects of exposure to tunicamycin, cells were cultured in the absence of FBS for extended periods of time. Deprivation of serum or exposure to tunicamycin led to apoptotic cell death, as verified by trypan blue inclusion and observation of nuclear morphology/integrity (Fig. 3). After induction of stress, WT LEC exhibited increased production of SPARC and a decreased apoptotic rate relative to SPARC-null LEC under similar conditions. Although not explored here, it is possible that alterations in protein glycosylation on SPARC or survival-related proteins could result in increased SPARC-mediated survival. Previous work in our laboratory has shown that alterations in glycosylation do not change SPARC function, but alterations to other proteins remain a factor for consideration.
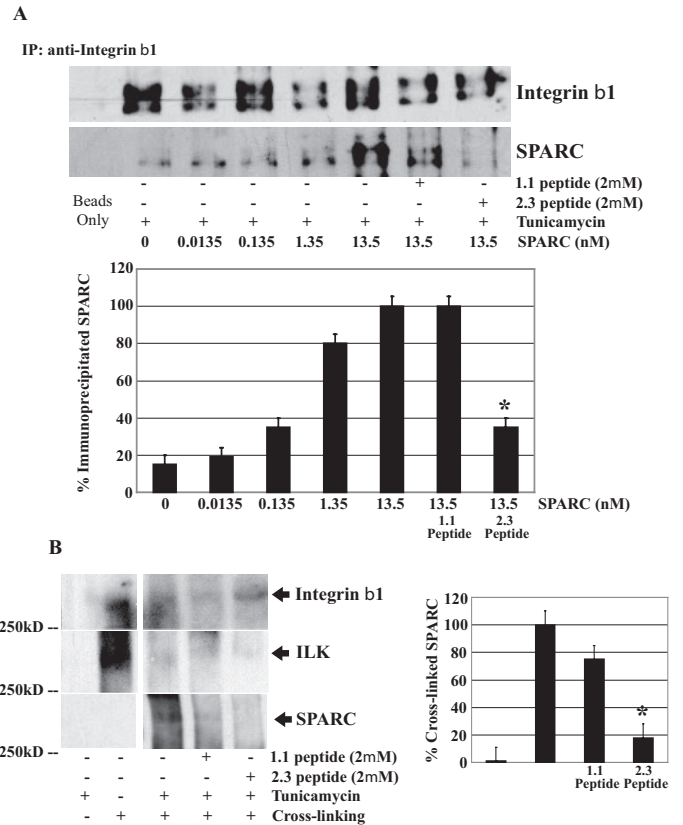
ILK signaling in the presence of SPARC was characterized by immunoblotting and immunocytochemistry. Immunoblots or staining of WT and SPARC-null LEC lysates after serum deprivation or exposure to tunicamycin (Fig. 4*A*) revealed enhanced ILK signal in both LEC lines. Whereas stress

stressed cells at least in part by its augmentation of downstream ILK activity through interaction with ILK-associated integrins β1/β3. Our results here indicate that cell death resulting from stress induction is apoptotic, as defined by nuclear morphology. Because we have not pursued additional apoptotic indicators or additional downstream ILK signaling, it is formally possible that cell death after stress is non-apoptotic. In either circumstance the role of SPARC is one of pro-survival during cellular response to stress.

As had been demonstrated previously, induction of stress in cultured cells increased expression of both SPARC and ILK, including increased secretion of SPARC into the culture medium (Fig. 1). In contrast to SPARC and ILK proteins, integrin β1 appeared to decrease with stress. However, subsequent

A

IP: anti-Integrin b1

A

IP: anti-Integrin b1

B

IP: anti-Integrin b1

FIGURE 11. **SPARC peptide 2.3 competes for SPARC-integrin β1 binding in a concentration-dependent manner.** WT LEC were subjected to serum deprivation (48 h) or tunicamycin (24 h) in the presence of SPARC peptide 2.3 or 1.1. *A*, co-immunoprecipitation (*IP*) of SPARC and integrin β1. Relative amounts of immunoprecipitated SPARC were normalized to the total amount of integrin β1 immunoprecipitated in each sample. *B*, specific, concentration-dependent inhibition of SPARC-integrin β1 interaction by SPARC peptide 2.3. In *A* and *B*, data were normalized to immunoprecipitated integrin β1, and each *column* represents the mean of three independent experiments ±S.D. Singular and composite blots are from single membranes and are representative of three independent experiments.

B

FIGURE 12. **SPARC peptide 2.3 inhibits extracellular SPARC interaction with integrin β1.** Lysates of SPARC-null LEC treated with tunicamycin (24 h) in the presence of SPARC (0–13.5 nM) with and without SPARC peptides (1.1 or 2.3) were immunoprecipitated (*IP*) by rabbit anti-integrin β1 IgG. Lysates of tunicamycin-stressed (24 h) WT LEC with and without SPARC peptides (*1.1* or *2.3*) were subsequently cross-linked. Immune complexes and cross-linked proteins were probed for SPARC, ILK, and integrin β1 by immunoblot as indicated. *A*, co-immunoprecipitation (*IP*) of SPARC and integrin β1. Relative amounts of immunoprecipitated SPARC were normalized to the total amount of integrin β1 immunoprecipitated in each sample. *B*, immunoblot of SPARC, ILK, and integrin β1 in cross-linked protein complexes from WT LEC with and without tunicamycin treatment and SPARC peptides. Singular and composite blots are from a single membrane and are representative of three independent experiments. In *A* and *B*, data were normalized to immunoprecipitated integrin β1, and each *column* represents the mean of three independent experiments ±S.D. (*, $p < 0.05$).

increased protein levels of ILK in both WT and SPARC-null LEC, ILK activity was seen only in WT LEC (Fig. 4*B*). Further analysis revealed that inhibition of PI3K eliminated all the SPARC-mediated ILK activity in cultured LEC (Fig. 4*B*). Additionally, ILK-specific inhibition eliminated the survival advantage of WT LEC relative to their SPARC-null counterparts, whereas inhibition of ILK did not affect the survival of SPARC-null LEC (Fig. 5). These results indicate a specific, PI3K-dependent role for ILK activity in the anti-apoptotic function of SPARC.

SPARC affects adhesion *in vitro* in part by its disruption of focal adhesions and the binding of integrins to ECM components (14). The cytoplasmic tails of integrins β1/β3 bind to ILK and in turn modulate its activity (22). We, therefore, asked whether integrins could bridge signaling between extracellular SPARC and intracellular ILK. After stress induction in the absence of serum or in the presence of tunicamycin, there was a significant increase in SPARC protein that was co-immunoprecipitated with integrin β1 in WT LEC (Fig. 6*A*). Immunopre-

cipitation of integrin β1 from SPARC-null cells exposed to WT-conditioned medium also isolated interacting SPARC protein under stress conditions. The SPARC-integrin β1 interaction appears to be specific, as several anti-integrin β1 antibodies recognizing different epitopes produced similar results (Fig. 6*B*). Elimination of SPARC-integrin β1 interaction via periodic removal of conditioned media demonstrated that secreted SPARC is required for the observed complex formation. This finding validates an extracellular connection between the SPARC and integrin β1 (Fig. 6*C*). Finally, protein cross-linking revealed a large, cell-associated complex containing ILK and integrin β1, and induction of stress resulted in the inclusion of SPARC in this complex (Fig. 6*D*).

We propose that the SPARC protein co-immunoprecipitated with anti-ILK antibodies during stress and/or during fibronectin assembly is in a complex with ILK and integrin β1. These findings do not eliminate the possibility that ILK and SPARC have direct interaction at the cell surface, but they do indicate a

IP: anti-ILK
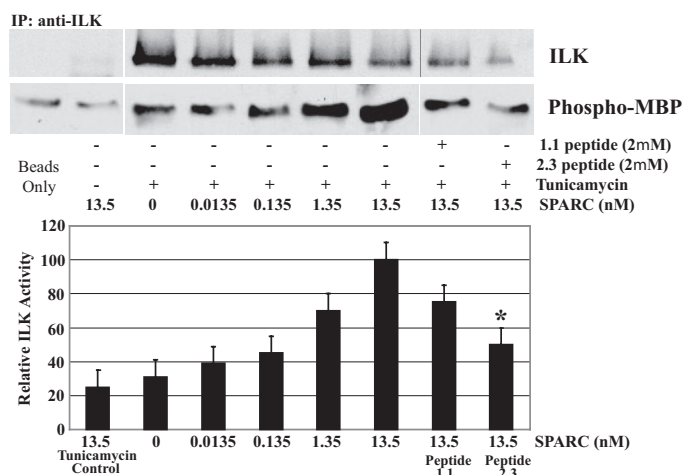
FIGURE 13. **SPARC peptide 2.3 inhibits SPARC-induced ILK activity.** SPARC-null LEC were treated with tunicamycin (24 h) in the presence of SPARC (0–13.5 nм) with and without SPARC peptides (*1.1* or *2.3*). Lysates were co-immunoprecipitated (*IP*) with rabbit anti-ILK antibodies and assayed for ILK activity. Relative expression of ILK in WT cells under each condition was normalized to the total amount of ILK protein immunoprecipitated for each reaction. Composite blots shown are from a single membrane and are representative of three independent experiments. Data were normalized to immunoprecipitated integrin ILK, and each *column* represents the mean of three independent experiments ±S.D. (*, $p < 0.05$).

role for integrins in SPARC-mediated signaling, as a functional interface between ILK and SPARC.

The use of anti-SPARC mAbs or a function-blocking anti-integrin β1 antibody eliminated SPARC from the immunoprecipitated complex before and especially after stress induction (Fig. 8*A*; Fig. 7*A*). Blocking of a SPARC-integrin β1 interaction impaired both downstream ILK activation (Fig. 7*B*) and survival of WT LEC under stress (Fig. 8*B*). These results confirm that stress-induced SPARC-ILK signaling is mediated at least in part by integrin β1 *in vitro*. The antibodies we used to immunoprecipitate and block integrin β1 impair the adhesive function of this integrin. Because active integrins are required for functionality on the cell surface, we conclude that SPARC forms a complex primarily with the active form of integrin β1 on the cell surface. These findings do not preclude the possibility that SPARC and integrin β1 do not directly interact. It is possible that additional cellular factors are required to mediate or enhance the SPARC-integrin β1 interaction demonstrated here.

To explain the varied success of the anti-SPARC mAbs to inhibit complex formation between integrin β1 and SPARC, we determined specific epitopes for each of the four mAb. Those mAb that inhibited the binding of SPARC to integrin β1 (236, 255, and 293; Fig. 8*A*) were shown to recognize epitopes in the follistatin domain of SPARC (Figs. 9 and 10). The capacity of each mAb to block SPARC appeared coincident with its reactivity with SPARC peptide 2.3 (27, 32). Competition assays showed that SPARC peptide 2.3 was capable of specific, concentration-dependent inhibition of SPARC-integrin β1 interaction (Fig. 11). Further analysis indicated peptide 2.3 was capable of inhibiting (i) the integrin β1 binding, (ii) the integrin-ILK complex formation, and (iii) and the ILK signaling conferred by extracellular SPARC on stressed LEC (Figs. 12 and 13).

Peptide 2.3 represents a copper binding sequence that stimulates angiogenesis via its enhancement of the endothelial cell cycle (27, 39). KKGHK can be proteolytically released (with flanking amino acids) from SPARC after degradation by extracellular proteases associated with wound repair and tissue remodeling *in vivo* (27, 32). It is plausible that during injury, development, tissue remodeling, and/or stress *in vivo*, the localized increase in SPARC protein results in an interaction with integrin β1 in which intact SPARC or SPARC proteolytic fragments participate. Subsequently, the pro-survival and angiogenic signaling required for the resolution of injury would occur. In conclusion, SPARC has an ILK-dependent, anti-apoptotic function in cultured LEC that is dependent on its copper binding domain mediating interaction with integrin β1.

Note added in Proof—The final version of this paper differs from the Papers in Press version in that the graphics for some of the figures initially did not comply with the JBC requirements. Specifically, individual portions of composite gels were not clearly delineated. The data in the paper have not been changed.

REFERENCES

1. Gilmour, D. T., Lyon, G. J., Carlton, M. B., Sanes, J. R., Cunningham, J. M., Anderson, J. R., Hogan, B. L., Evans, M. J., and Colledge, W. H. (1998) *EMBO J.* **17,** 1860–1870
2. Norose, K., Clark, J. I., Syed, N. A., Basu, A., Heber-Katz, E., Sage, E. H., and Howe, C. C. (1998) *Investig. Ophthalmol. Vis. Sci.* **39,** 2674–2680
3. Norose, K., Lo, W. K., Clark, J. I., Sage, E. H., and Howe, C. C. (2000) *Exp. Eye Res.* **71,** 295–307
4. Yan, Q., Clark, J. I., Wight, T. N., and Sage, E. H. (2002) *J. Cell Sci.* **115,** 2747–2756
5. Yan, Q., Blake, D., Clark, J. I., and Sage, E. H. (2003) *J. Histochem. Cytochem.* **51,** 503–511
6. Bradshaw, A. D., Reed, M. J., and Sage, E. H. (2002) *J. Histochem. Cytochem.* **50,** 1–10
7. Kyriakides, T. R., and Bornstein, P. (2003) *Thromb. Haemostasis* **90,** 986–992
8. Puolakkainen, P. A., Bradshaw, A. D., Brekken, R. A., Reed, M. J., Kyriakides, T., Funk, S. E., Gooden, M. D., Vernon, R. B., Wight, T. N., Bornstein, P., and Sage, E. H. (2005) *J. Histochem. Cytochem.* **53,** 571–581
9. Brekken, R. A., Puolakkainen, P., Graves, D. C., Workman, G., Lubkin, S. R., and Sage, E. H. (2003) *J. Clin. Investig.* **111,** 487–495
10. Puolakkainen, P. A., Brekken, R. A., Muneer, S., and Sage, E. H. (2004) *Mol. Cancer Res.* **2,** 215–224
11. Said, N., and Motamed, K. (2005) *Am. J. Pathol.* **167,** 1739–1752
12. Tartare-Deckert, S., Chavey, C., Monthouel, M. N., Gautier, N., and Van Obberghen, E. (2001) *J. Biol. Chem.* **276,** 22231–22237
13. Bradshaw, A. D., Graves, D. C., Motamed, K., and Sage, E. H. (2003) *Proc. Natl. Acad. Sci. U. S. A.* **100,** 6045–6050
14. Murphy-Ullrich, J. E. (2001) *J. Clin. Investig.* **107,** 785–790
15. Weaver, M. S., Sage, E. H., and Yan, Q. (2006) *J. Cell. Biochem.* **97,** 423–432
16. Sage, E. H., Tupper, J., and Bramson, R. (1986) *J. Cell. Physiol.* **127,** 373–387
17. Neri, M., Descalzi-Cancedda, F., and Cancedda, R. (1992) *Eur. J. Biochem.* **205,** 569–574
18. Sauk, J. J., Smith, T., Silbergeld, E. K., Fowler, B. A., and Somerman, M. J. (1992) *Toxicol. Appl. Pharmacol.* **116,** 240–247
19. Shi, Q., Bao, S., Maxwell, J. A., Reese, E. D., Friedman, H. S., Bigner, D. D., Wang, X. F., and Rich, J. N. (2004) *J. Biol. Chem.* **279,** 52200–52209

20. Shi, Q., Bao, S., Song, L., Wu, Q., Bigner, D. D., Hjelmeland, A. B., and Rich, J. N. (2007) *Oncogene* **26,** 4084–4094
21. Barker, T. H., Baneyx, G., Cardo-Vila, M., Workman, G. A., Weaver, M., Menon, P. M., Dedhar, S., Rempel, S. A., Arap, W., Pasqualini, R., Vogel, V., and Sage, E. H. (2005) *J. Biol. Chem.* **280,** 36483–93643
22. Attwell, S., Mills, J., Troussard, A., Wu, C., and Dedhar, S. (2003) *Mol. Biol. Cell* **14,** 4813–4825
23. Kzhyshkowska, J., Workman, G., Cardo-Vila, M., Arap, W., Pasqualini, R., Gratchev, A., Krusell, L., Goerdt, S., and Sage, E. H. (2006) *J. Immunol.* **176,** 5825–5832
24. Kzhyshkowska, J., Gratchev, A., and Goerdt, S. (2006) *J. Cell. Mol. Med.* **10,** 635–649
25. Weaver, M. S., Toida, N., and Sage, E. H. (2007) *Mol. Vis.* **13,** 707–718
26. Lane, T. F., and Sage, E. H. (1990) *J. Cell Biol.* **111,** 3065–3076
27. Lane, T. F., Iruela-Arispe, M. L., Johnson, R. S., and Sage, E. H. (1994) *J. Cell Biol.* **125,** 929–943
28. Sweetwyne, M. T., Brekken, R. A., Workman, G., Bradshaw, A. D., Carbon, J., Siadak, A. W., Murri, C., and Sage, E. H. (2004) *J. Histochem. Cytochem.* **52,** 723–733
29. Yan, Q., Weaver, M. S., Perdue, N., and Sage, E. H. (2005) *J. Cell. Physiol.* **203,** 286–294
30. Ikesugi, K., Yamamoto, R., Mulhern, M. L., and Shinohara, T. (2006) *Exp. Eye Res.* **83,** 508–516
31. Ribble, D., Goldstein, N. B., Norris, D. A., and Shellman, Y. G. (2005) *BMC Biotechnol.* 5:12
32. Sage, E. H., Reed, M., Funk, S. E., Truong, T., Steadele, M., Puolakkainen, P., Maurice, D. H., and Bassuk, J. A. (2003) *J. Biol. Chem.* **278,** 37849–37857
33. Szegezdi, E., Logue, S. E., Gorman, A. M., and Samali, A. (2006) *EMBO Rep.* **7,** 880–885
34. Gasiorowski, K., Brokos, B., Kulma, A., Ogorzalek, A., and Skorkowska, K. (2001) *Cell. Mol. Biol. Lett.* **6,** 141–159
35. Mills, J., Digicaylioglu, M., Legg, A. T., Young, C. E., Young, S. S., Barr, A. M., Fletcher, L., O'Connor, T. P., and Dedhar, S. (2003) *J. Neurosci.* **23,** 1638–1648
36. Yan, Q., Liu, J. P., and Li, D. W. (2006) *Differentiation* **74,** 195–211
37. Martinek, N., Shahab, J., Sodek, J., and Ringuette, M. (2007) *J. Dent. Res.* **86,** 296–305
38. Emerson, R. O., Sage, E. H., Ghosh, J. G., and Clark, J. I. (2006) *J. Cell. Biochem.* **98,** 701–705
39. Funk, S. E., and Sage, E. H. (1993) *J. Cell. Physiol.* **154,** 53–63
40. Hohenester, E., Maurer, P., and Timpl, R. (1997) *EMBO J.* **16,** 3778–3786